International Research Journal of
SCIENCE, TECHNOLOGY, EDUCATION, AND MANAGEMENT
P-ISSN: 2799-063X — E-ISSN: 2799-0648
Volume 4, No. 1 | March 2024

Numerical analysis of internal flow phenomena in a backward curved centrifugal fan

Khema Theint[1], War War Min Swe[2], Aung Kyaw Soe[3], Aung Ko Latt[4]
[1,2,3,4]*Mandalay Technological University, Myanmar*
Corresponding Email: khematheint.kmt@gmail.com

ABSTRACT

Centrifugal fans are widely used in applications for the ventilation of air to induce pressure and drive the flow medium. The centrifugal fans are applied not only to produce fresh air but also to absorb toxic gases from the environment. Complex flow patterns are present in the centrifugal fan's impeller and volute casing. The flow patterns of a backward curved centrifugal fan are the main topic of this study. The flow in the impeller blade channels needs to be better understood to optimize the design and performance of any turbomachine. This work uses numerical analysis to examine the flow patterns inside a backward curved centrifugal fan employed in the ventilation system. Computational fluid dynamic code serves as the foundation for numerical analysis, ANSYS-CFX 21.2. The fan under investigation in this study has an operational speed of 1500 rpm, a pressure head of 4 m, and a volume flow rate of 3 m^3min^{-1}. A change in mass flow rates has a direct impact on the pressure and velocity distributions in the centrifugal fan's impeller passageways. By varying the mass flow rates, the numerical results have demonstrated the three-dimensional properties of the flow, particularly in the impeller blade passageways and the casing. The fan casing contains the high-pressure region, while the impeller intake is the low-pressure area. The area within the volute tongue in which flow recirculation occurs. The backward curved centrifugal fan has a static efficiency of 93% and a total efficiency of 96% at the specified volume flow rate. This suggested methodology can be used to identify fluid flow constraints in the volute casing, comprehend internal flow patterns in the backward curved centrifugal fan, and enhance centrifugal fan performance.

ARTICLE INFO

Received : Feb. 19, 2024
Revised : Mar. 9, 2024
Accepted : Mar. 31, 2024

KEYWORDS

Backward curved centrifugal fan, CFD-CFX, Internal flow phenomena, Mass flow rate

Suggested Citation (APA Style 7th Edition):

Theint, K., Swe, W.W.M., Soe, A.K., & Latt, A.K. (2024). Numerical analysis of internal flow phenomena in a backward curved centrifugal fan. *International Research Journal of Science, Technology, Education and Management*, 4(1), 22-39. https://doi.org/10.5281/zenodo.10972028

INTRODUCTION

The impeller blades of a centrifugal fan are positioned between the inner and outer diameters. Air enters the impeller axially in a centrifugal fan, is accelerated by the blades, and is released radially. The impeller's motion causes the gas to swing between smaller and bigger diameters, delivering high pressure and velocity to the casing. The stage pressure rises according to the centrifugal energy. A scroll, also called a volute, is a spiral-shaped casing that collects the flow from the impeller blades. It sends the air to the fan's exit. The air's static pressure can be further raised by the scroll case. Conical diffusers are another possible shape for the outlet route that follows the scroll (Yahya, S. M. 2011).

In this work, a backward curved centrifugal test fan consists of the following components. These are the backward curved impeller, the volute casing, the buffer, and the wind duct. A buffer is a place that meets the casing exit and wind duct inlet. The assembly of the backward curved centrifugal fan is presented Fig.1.

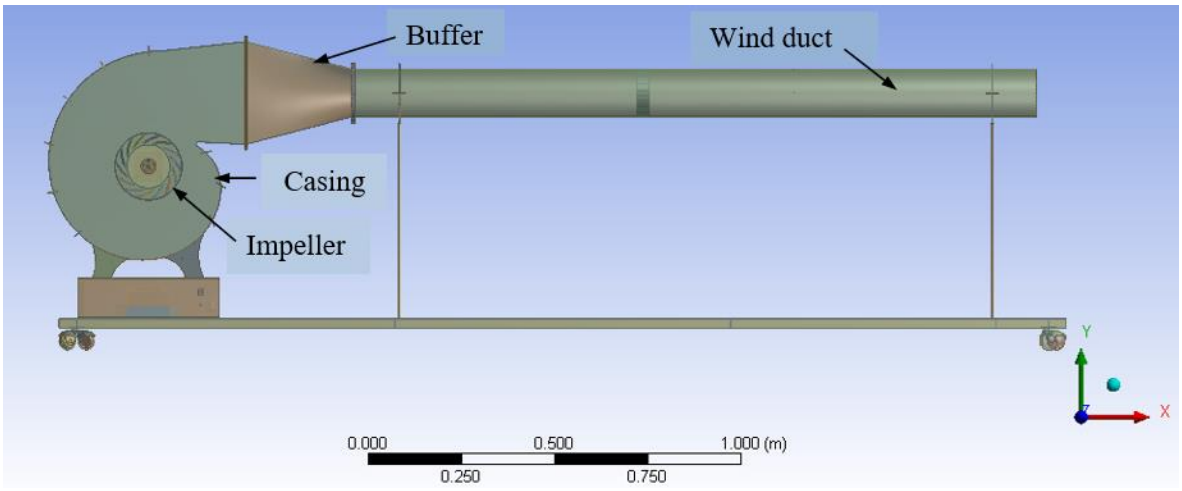

Figure 1. Backward curved centrifugal fan

Previous studies have attempted to determine the centrifugal fan's internal flow patterns. In earlier studies, Wang, J. (2005) created computational fluid dynamics (CFD) models for turbulent flow fields in an air conditioner's multi-blade centrifugal fan. The computational results have demonstrated the three-dimensional characteristics of the flow, especially in the impeller blade passageways near the shroud side. The findings have shown various characteristics of the flow, including its reversal from the high-pressure region in the volute casing to the low-pressure region near the impeller entry, its recirculation near the shroud side, a jet-wake pattern at the rotor exit, pressure variations on the blade surface. Additionally, a boundary layer divides the flow and the leading edge of the blade suction surface.

The effects of a straight shroud with different inclined degrees on the fan's performance were studied by Liu, X., et al. (2008). The investigator concluded that every impeller path had a distinct flow. According to the final data, the circular flow that forms in the shroud outside is what causes the leakage loss. The flow must be redirected to the volute casing's upstream side concurrently. According to the author, there is non-uniformity in the flow characteristics around the impeller outlet, the volute inlet, and the interaction between the impeller blades and the volute.

The aerodynamic performance of centrifugal fans under the impact of fan casing geometries was reported by Swe et al. in (2019). For the centrifugal fan, fan housing, and impeller blades, the flow parameters

and energy loss are examined. The authors arrived at the conclusion that, as compared to a scroll casing fan, the fan with rectangular casing exhibits better flow performance characteristics, resulting in an improved over-design flow rate. According to their report, the scroll casing loses more energy than the rectangular casing. The scroll casing has a significant energy loss, particularly in the outlet casing.

Gjeta et al.'s research study from (2020) reviewed the effect of the spiral casing design's outlet surface area on the centrifugal fan's performance. Steady and unsteady simulations for a rectangular fan casing were discussed by Swe, W. W. M., Hayashi, H., Okumura, T., Morimatsu, H., & Oda, I. (2017). It was found that the fan performances' results were unrelated in both steady and unstable simulations. The authors (Huang et al., 2013) discussed the inverse design problem of the optimal three-dimensional form of a centrifugal-flow fan based on the intended airflow rate.

After observing the Euler approach, Abbitt et al. (2016) used SolidWorks to generate a digital model and set up a computational fluid dynamic to optimize their design. In 2014, Brahmbhatt, V., and Patel, G. investigated the centrifugal fan system design methods utilizing impellers. To improve the results obtained by the numerical method, the authors solved the numerical simulation and performed CFD optimization for volute casing.

Singh et al., (2011) examined the impact of geometric parameters on a centrifugal fan featuring blades that bend both forward and backward. First, each author took the study's parameters into account. These were the diameter ratios, outlet angles, and blade count. The authors explain that a rise in the power coefficient and a fall in efficiency follow a rise in the flow coefficient. It was discovered that, when the pressure coefficient was large, fans with various blade configurations performed similarly.

Nearly all cases involving scroll casing have been studied regarding backward curved centrifugal fans. The backward curved centrifugal fan's performance analysis was visualized by Yokoi et al. (2005), Yu et al. (2005), and Chaudhary et al. (2013). This analysis searches into the way various blade angles affect the fan's static pressure and overall pressure. It is appropriate to use this research to select the fan type.

The effect of the volute spread angle on the squirrel cage fan's efficiency, performance, and flow pattern was investigated experimentally and numerically by Samarbakhsh et al. (2011). A volute's flow is quite complicated. It is firmly believed that by identifying the process responsible for entropy formation, a complete understanding of the flow structure within a volute will offer valuable insights into decreasing losses. Eight volutes with slightly different volute profile equations are investigated both computationally and experimentally for the study that is being presented here. Both the velocity components and the fans' total performances were measured. The writers demonstrated how to be efficient in a small area without sacrificing the intended mass flow rate.

The design techniques, performance, and efficiency of fans were the primary focus of all of the previous studies. Several studies and numerical simulation techniques have been tried by numerous researchers in an effort to forecast and enhance fan performance. Furthermore, the pressure gradients and velocity fields inside the centrifugal fan have been successfully detected by this research effort. This idea can be used by the new researchers to approach the fan's new design techniques.

This research aims to examine the internal flow phenomena of the backward centrifugal fan by changing mass flow rates. Computational fluid dynamics is also the foundation of flow analysis, which provides findings for the estimation of the velocity distribution and pressure fluctuation for the centrifugal fan with a reverse curve. The main challenge is the interacting flow between the impeller blades and the casing, according to the results of the simulation, analysis, and comparison. Understanding the flow behavior in a centrifugal fan with a curve that is reversed and increasing fan efficiency are the goals of this effort.

Backward Curved Centrifugal Impeller

The design of backward curved centrifugal impeller is intended for the head H = 4 m, the volume flow rate, Q = 3m^3/min, and the motor speed, N = 1500 rpm. The input parameters are impeller inlet diameter is 128 mm, outlet diameter is 178 mm, blade inlet angle is 23º, blade outlet angle is 30º, span height is 30 mm, blade thickness is 2mm and blade length is 55 mm. Fig 2. demonstrates the backward curved centrifugal impeller blade profile.

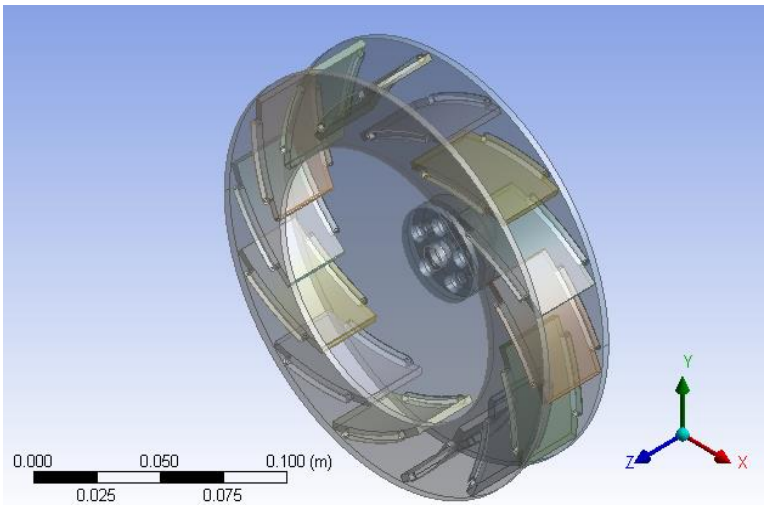

Figure 2. Backward Curved Centrifugal Impeller Blade

THE APPROACH FOR THE NUMERICAL ANALYSIS

In this numerical study, the numerical analysis code ANSYS-CFX 21.2 software was used to analyze the internal flow of the centrifugal fan. The CFD programs gain more importance for the design and analysis of fluid turbomachines during operation and also provide invaluable insight, as to how the turbomachines operate and how it might be improved. The predetermined performance was conducted from the simulation results. The simulations were done for steady-state and transient. The most important part of CFD analysis is to define the fluid properties and boundary conditions. The simulation work includes geometry creation, mesh generation, and convergence of fluid domain. In this study, the geometry is constructed in an ANSYS-CFX workbench. The impeller, the volute casing, and the wind duct are created and assembled. After creating the model, meshing is also done in CFD-CFX itself. To analyze the flow through numerical simulation, the backward curved centrifugal fan is used which is run by a motor having a rotational speed of 1500 rpm by rotating the clockwise direction of the impeller. The impeller blade consists of fourteen 3-D backward curved blades with an exit angle of 30° relative to the tangential direction.

The test fan comprises the two parts: stationary part and rotating part. The stationary part such as the casing and the wind duct, and the rotating part such as the impeller. The flow characteristics were analyzed at impeller inflow and outflow, inside the casing, and the centrifugal fan to different eight mass flow rates.

Creating the Domains

Three domains that were created in ANSYS 21.2 Workbench. There was an inlet domain, a rotating domain, and an outlet domain (see Fig 3). Inlet and outlet domains were stationary domains. The impeller is rotated at 1500 rpm, it is created as the rotating domain.

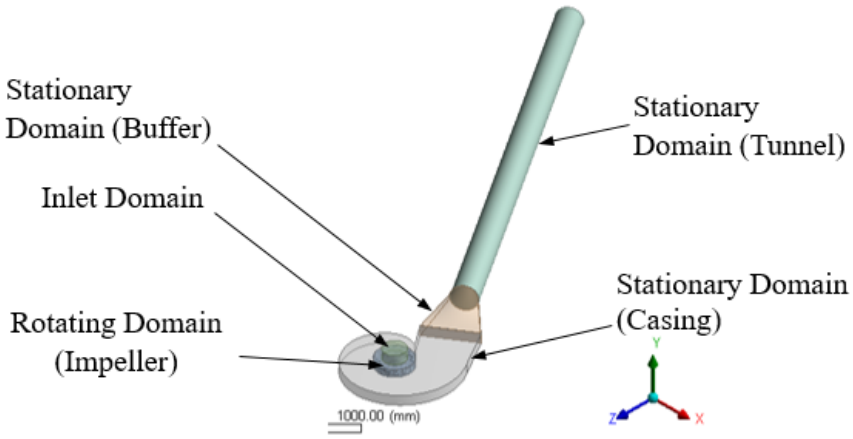

Figure 3. Creating of fluid domains

Generating Mesh

Meshing is employed to discrete the centrifugal fan computational domains by using ANSYS-CFX 21.2. The inflation mesh is used for the impeller blade and the volute casing. The first layer thickness option creates constant inflation layers by using the first layer height is 1 mm, maximum layer is 5, and growth rate is 1.2 controls to generate the inflation mesh. The fluid model is generated by the Tetrahedron mesh. The total number of nodes is 455512 and the total elements for all domains are 923728. The meshing of the fluid domain is denoted in Fig 4 (a) and (b).

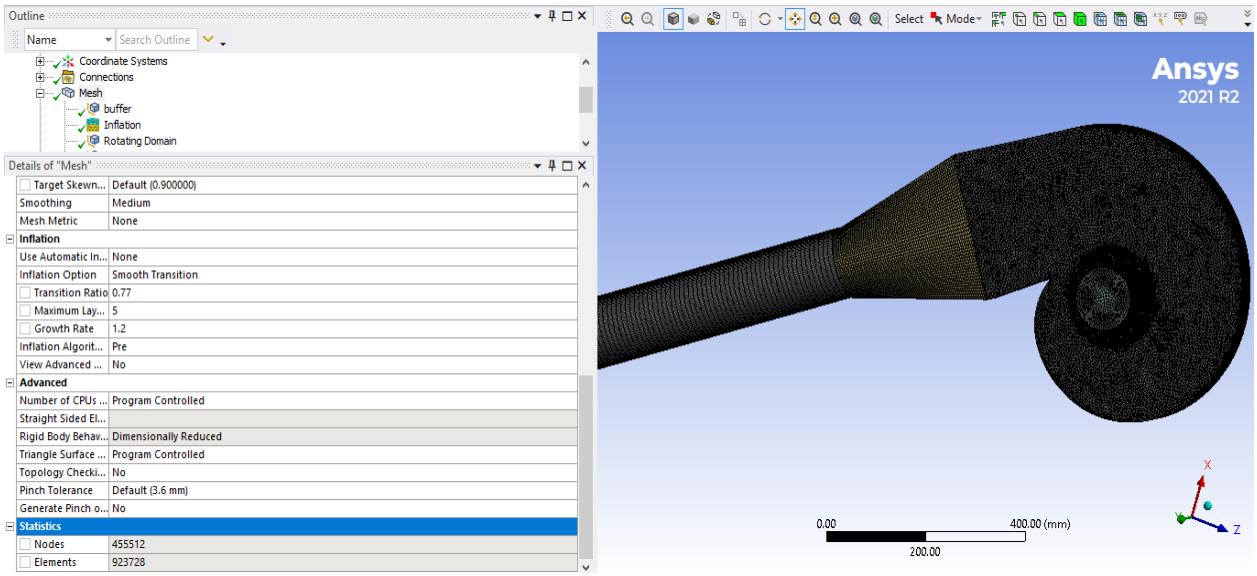

(a) Meshing of rotating and stationary domains

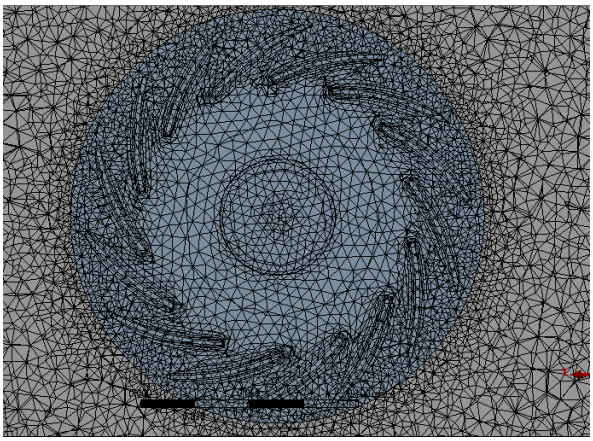

(b) Detail around the blade mesh

Figure 4. Mesh mode

Boundary Conditions

To examine the fan's flow state, the Reynolds averaged Navier-Stokes equations are used to model a steady flow. Shear stress transfer (SST) turbulence models serve as the foundation for the k-ω computational models. The input, the rotation, and the outflow are constructed by the computational domains. These domains are fluid, with air at 25°C serving as the working fluid. The atmospheric pressure (1 atm) serves as the reference pressure. Both the exit and the inlet domains are fixed. At 1500 rpm, the impeller rotates in a clockwise motion. The mass flow rate is in the outlet domain, and the static pressure is 0 Pa at the inlet domain. The boundary plane separating the impeller and casing areas is where the Frozen-Rotor interface is defined. Smooth walls and non-slip walls are illustrations of solid surfaces. Fig.5 shows the boundary condition for the test fan.

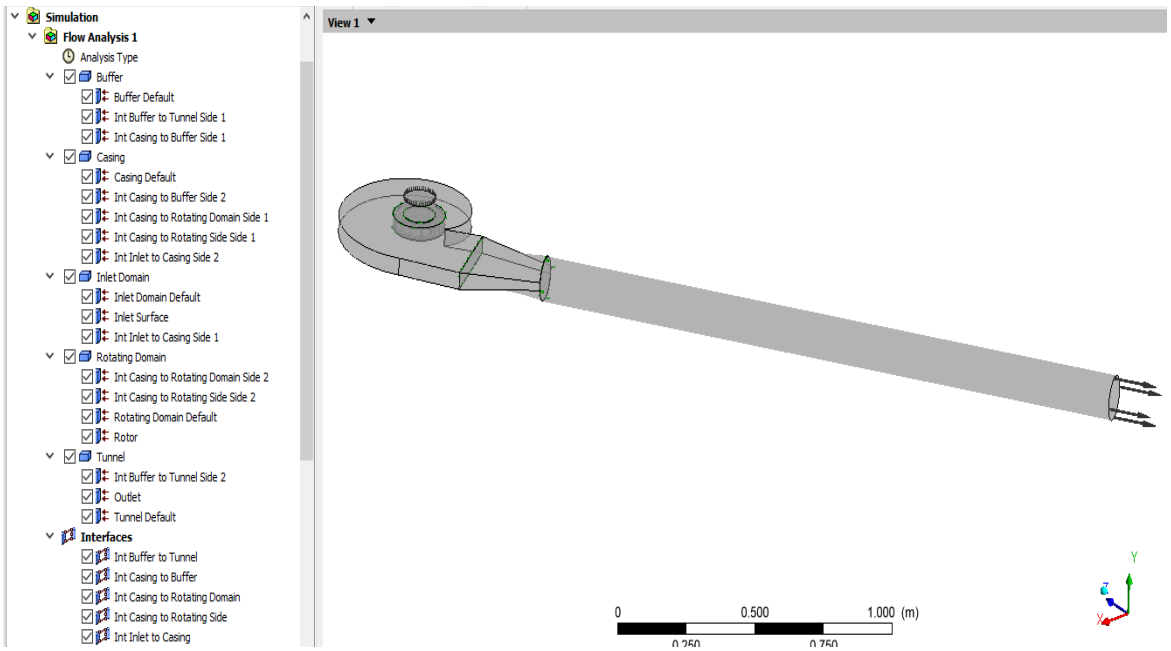

Figure 5. Setup boundary condition

Numerical Analysis

In this procedure, the input data are the pressure head of 4 m, the volume flow rate of 3 m^3/min, and the rotational speed of 1500 rpm. In this work, the steady-state calculations were done for eight mass flow rates. They are the flow rate coefficients of ϕ = 0.16, 0.18, 0.2, 0.22, 0.24, 0.26, 0.28, and 0.3, and the design flow coefficient is 0.22. The results of the flow analysis for different mass flow rates are presented along with the velocity and pressure distribution of the impeller passages.

Fan's Performance Curve

A plot of expanded pressure and power required over a range of fan-generated airflow is a standard way to define the performance of a fan (Gustafson, B., 1989). An understanding of the fan operating mechanism was necessary for the relationship. The performance of the fan is graphically represented in that work in terms of static pressure, total pressure, static efficiency, and total efficiency. The steady-state calculations for eight distinct mass flow rates were performed in that study. The volume flow rate was calculated according to equation (1). The static efficiency was calculated according to equation (2) and the total efficiency was calculated by equation (3). In equation (2), the input power was blade load and the output power was the static pressure increase from the impeller blades inlet to outlet. In equation (3), the input power was blade load and the output power was the total pressure increase from impeller inlet to outlet.

$$Q = AV_f \quad (1)$$

$$\eta_s = \frac{\Delta P_s Q}{T\omega} \quad (2)$$

$$\eta_t = \frac{\Delta P_t Q}{T\omega} \quad (3)$$

Where, Q = the air flow rate [m^3/s].
A = the impeller outlet area [m^2].
V_f = the velocity [m/s].
ΔP_s is the average static pressure [Pa].
ΔP_t *is* the average total pressure [Pa].
T = the impeller torque [N-m].
ω = the angular velocity of the impeller [rad/s].
η_s is the static efficiency [%].
η_t is the total efficiency [%].

Internal Flow Characteristics

The test fan's flow characteristics are initially determined utilizing the design flow rate. As seen in Fig. 6, three planes are built by Plane 1, Plane 2, and Plane 3 to assess the relative velocity, absolute velocity, static pressure, and total pressure of the flow inside the impeller and the casing. Fig.7 (a) to (c) depicts the velocity vectors in each plane. Fig.8 (a) to (c) implies the absolute velocity contours in each plane. Fig.9 (a) to (c) shows the static pressure contours diagram in each plane. Fig. 10 (a) to (c) demonstrates the total pressure contour map in each plane.

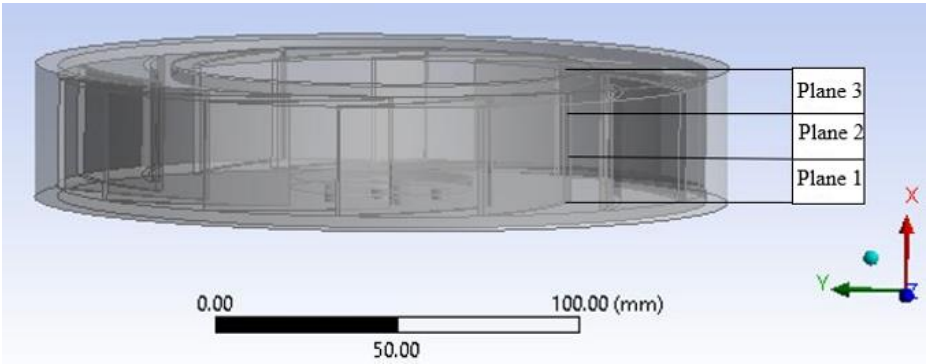

Figure 6. Locations for three planes

The velocity vectors in the volute casing are shown in Fig 7. (a) to (c). In Plane 1, the flow inside the impeller is smoothly matched on the impeller blades. The velocity vectors direct the usual flow direction. There is no backflow occurring in the tip clearance region. But at Plane 2 and Plane 3, some of the air is collected at the rear corner and side wall of the scroll casing. The fan outlet section's velocity vectors are essentially the same in all planes. Low velocity was seen at the wall of the volute in Fig.7 (a) through (c).

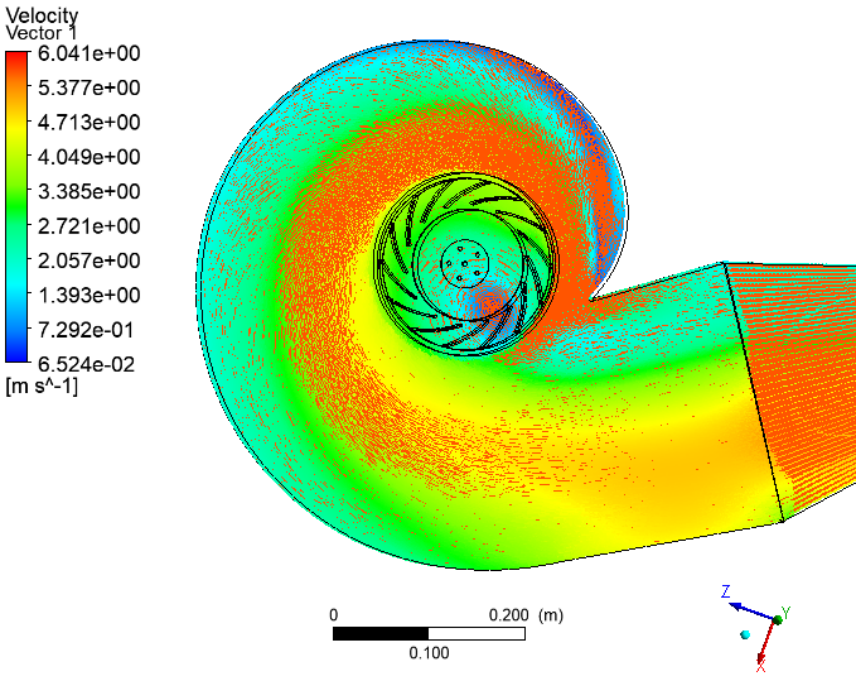

Figure 7. (a) Velocity vectors at Plane 1

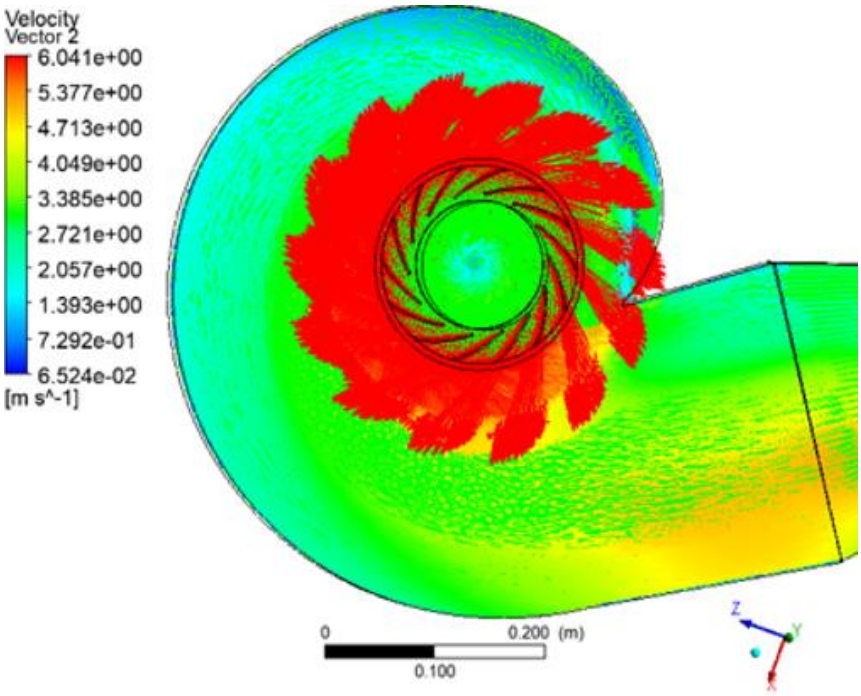

Figure 7. (b) Velocity vectors at Plane 2

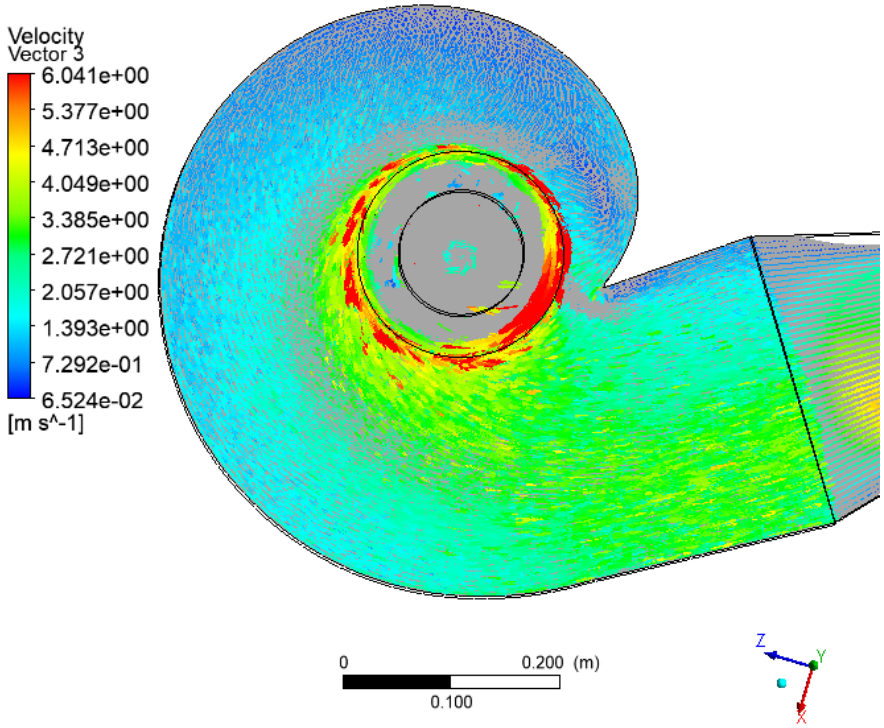

Figure 7. (c) Velocity vectors at Plane 3

The absolute velocity distribution of the fan at each plane is compared in Fig. 8(a) through (c). The blades' rotational region contains vortices. In Fig. 8(b), these vortices are visible. At the blades, there are

distinct vortices. In the wind duct section, the fan's absolute velocities are continuously low. The range of absolute velocities' numerical results is 0.065 m/s to 7.98 m/s.

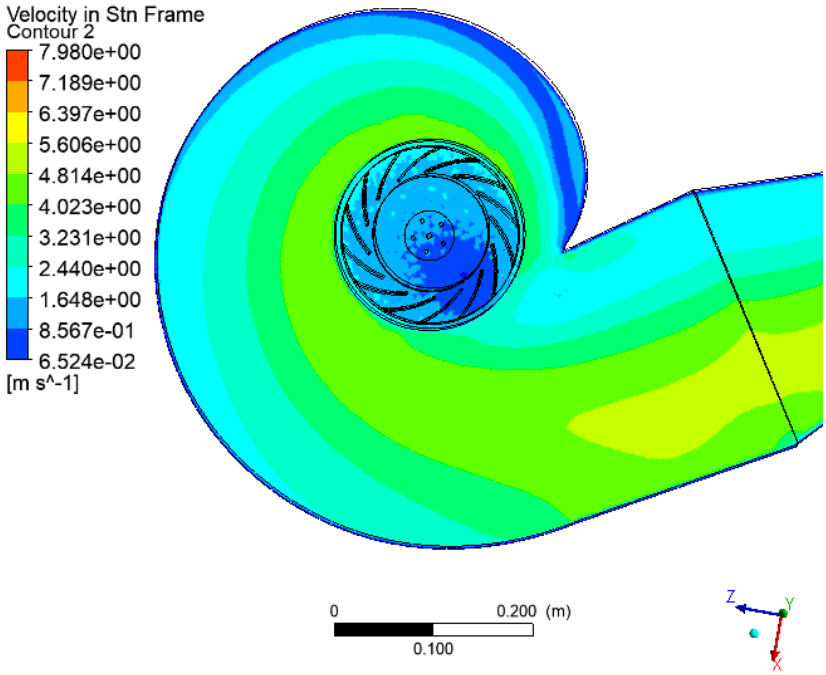

Figure 8. (a) Absolute velocity contours at Plane 1

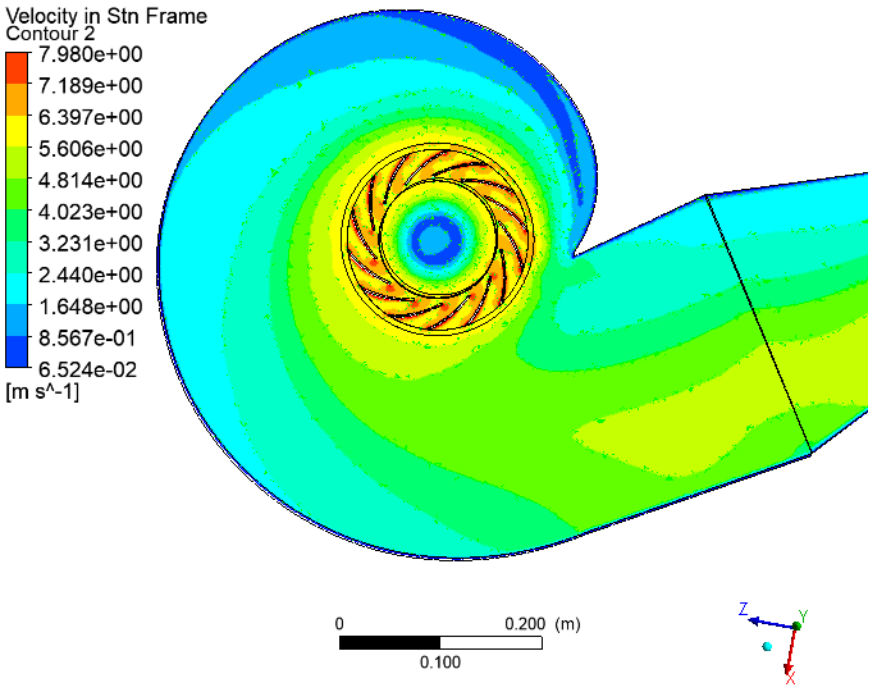

Figure 8. (b) Absolute velocity contours at Plane 2

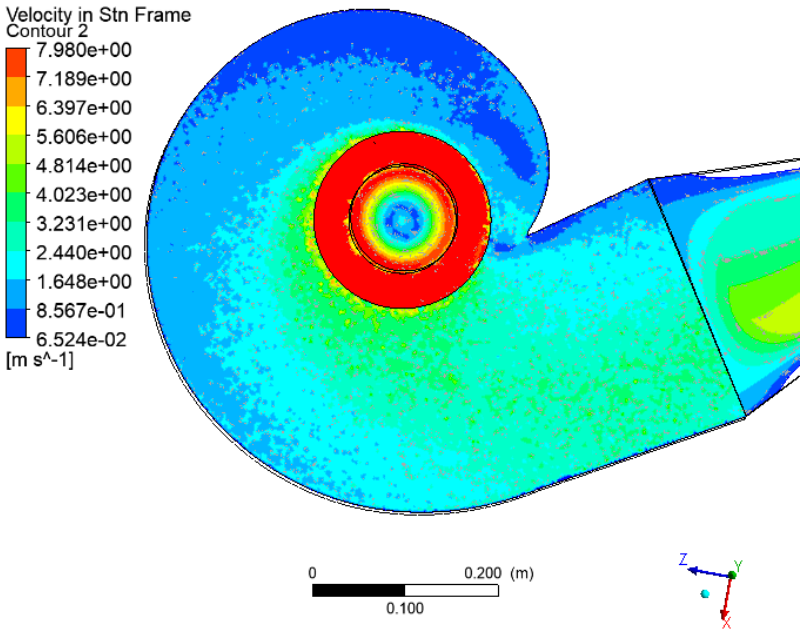

Figure 8. (c) Absolute velocity contours at Plane 3

Fig 9. (a) to (c) presents the pressure contour map at each plane. The figures illustrate that there is low static pressure within the fan's impeller blades. Subsequently, as the fluid particles pass through the impeller tip and into the fan casing, the pressure gradually increases. The pressure distributions at the fan exit are nearly similar in all planes. The simulation results of static pressure are in the range of 21.84 Pa to 52.36 Pa.

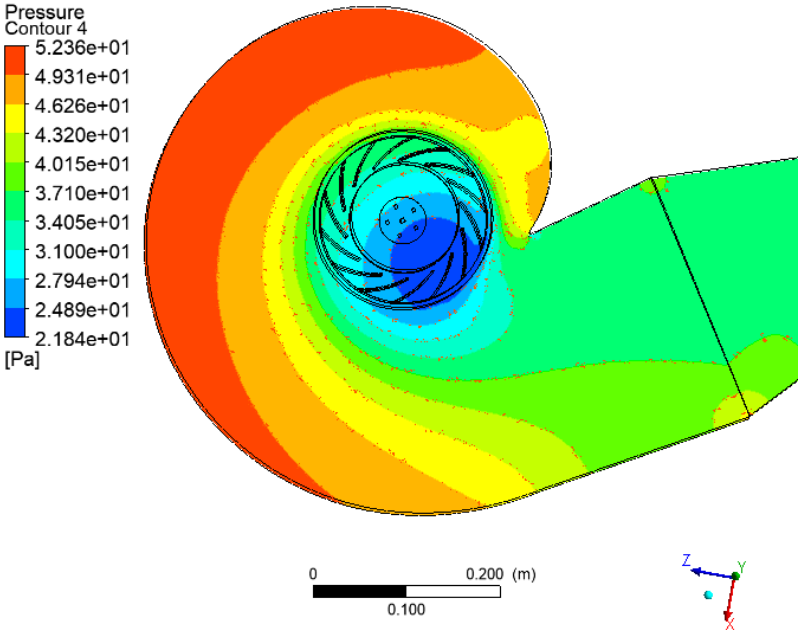

Figure 9. (a) Static Pressure Contours at Plane1

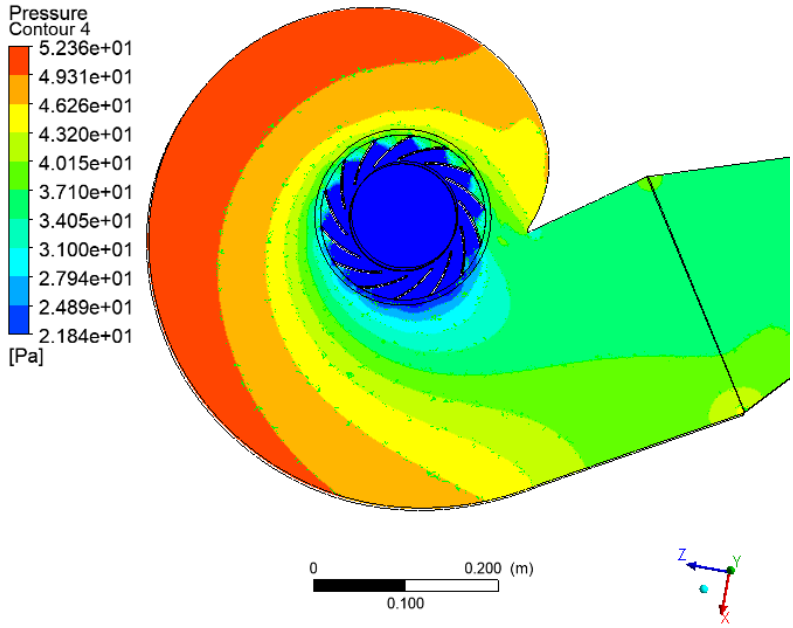

Figure 9. (b) Pressure Contours at Plane 2

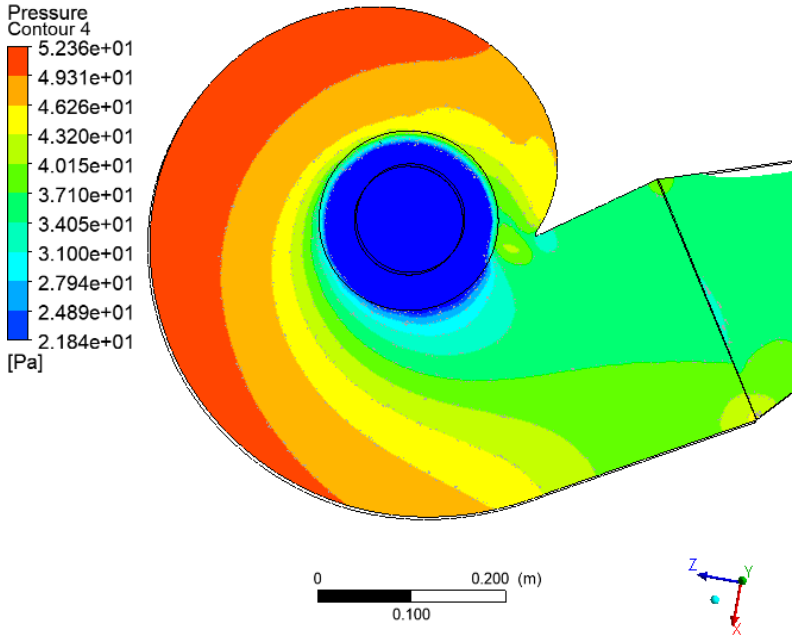

Figure 9. (c) Pressure Contours at Plane 3

Total pressure contours at each plane in the design flow rate are shown in Fig.10 (a) through (c). The hue of the contour is seen as the lowest pressure for the entire domain at the suction side. At the impeller blades' exit, the pressure is at its highest. A comparison of the three planes reveals that the high-pressure contours are observed around the tip region in the impeller. Variation in contours in Plane 1 is more than the other planes of the centrifugal fan. The simulation results of total pressure are in the range from 21.84 Pa to 57.24 Pa.

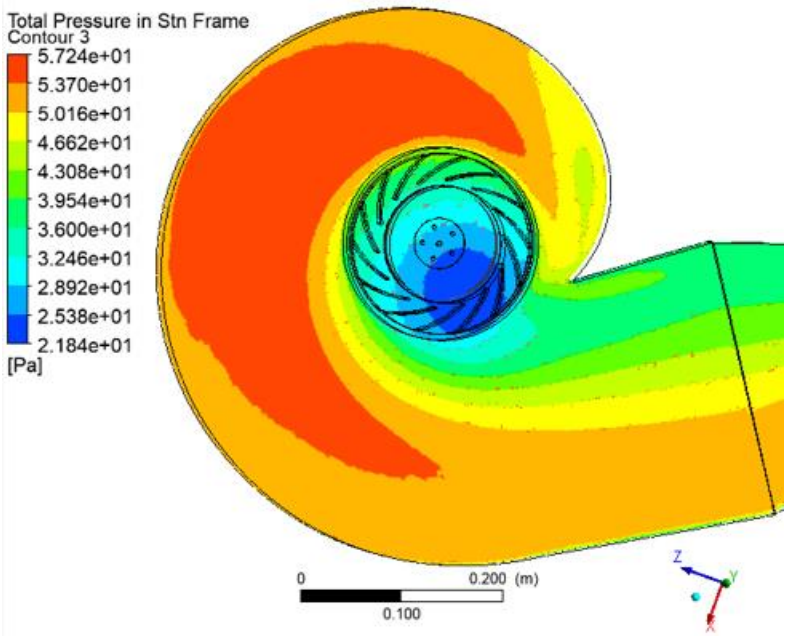

Figure 10. (a) Total pressure contours at Plane 1

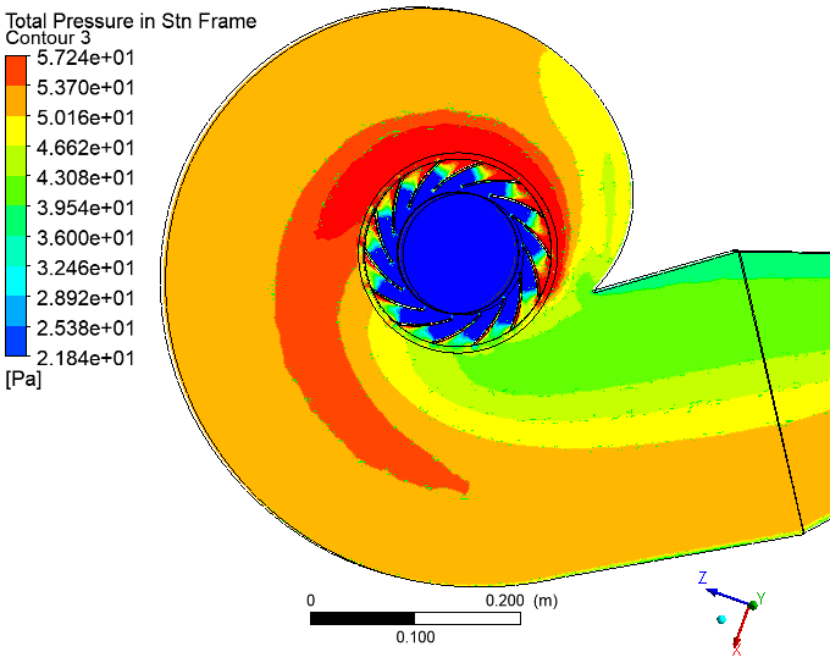

Figure 10. (b) Total pressure contours at Plane 2

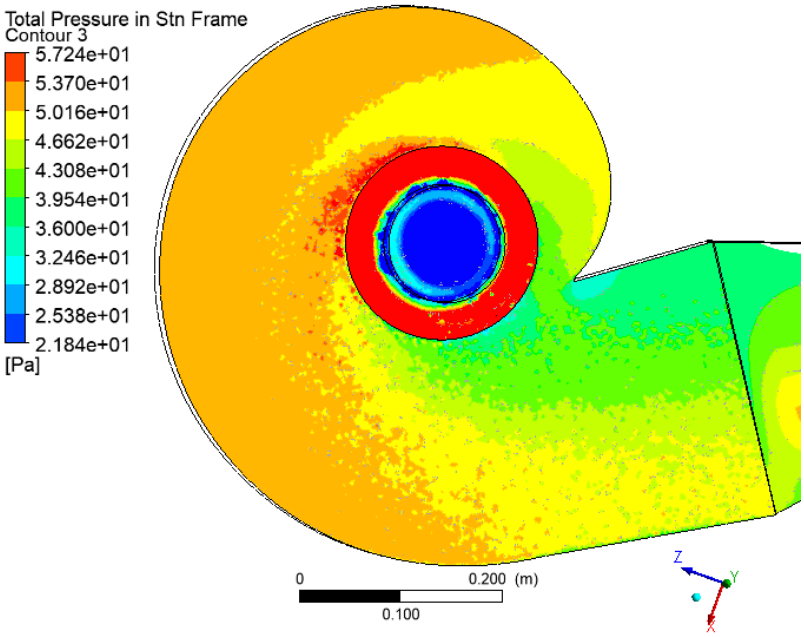

Figure 10. (c) Total pressure contours at Plane 3

As indicated in Fig. 11, the volute casing is split into six sections to conduct an airflow study within the casing. The centrifugal force produced by the impeller's rotation is the force that drives the centrifugal fan. The fluid particles are thrown away radially in the direction of the fan's volute casing by the impeller as it rotates. As a result, the area near the impeller tip displays high fluid particle velocity. Between the fan casing and the impeller, an abundance of air is gathered. A portion of the fluid is cycled within the centrifugal fan's housing. This area has recirculating flow due to tongue occlusion (Fig. 11).

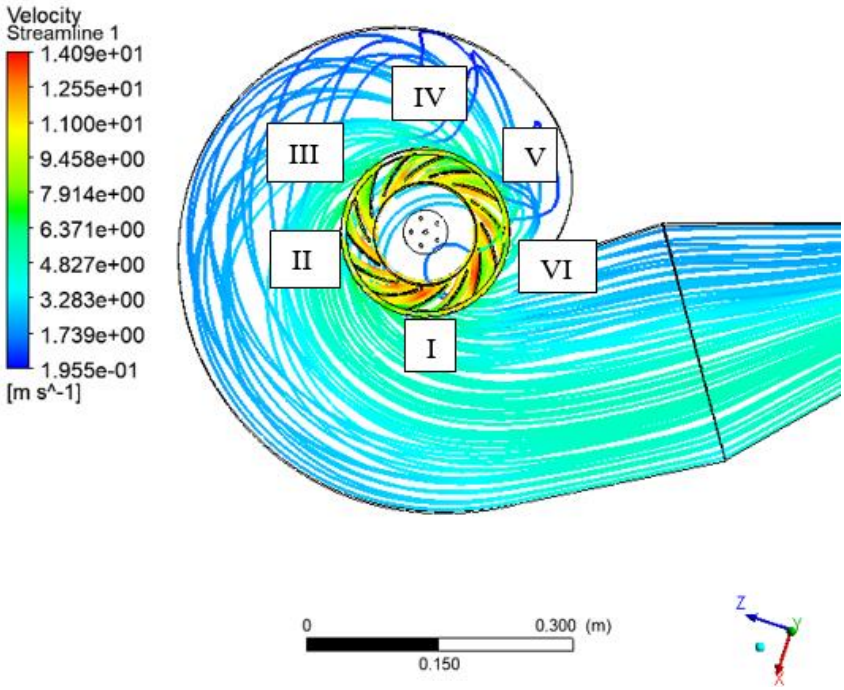

Figure 11. Velocity streamlines of test fan

The test fan's pressure distribution at the intended flow rate is shown in Fig. 12. At the outside circumference of the impeller, the static pressure rises (see Fig. 12). Near the fan's casing corner, where there is a low flow field, is where the static pressure is at its strongest (see Fig. 11. section V). As a result, the low flow zone is where the static pressure is strongest.

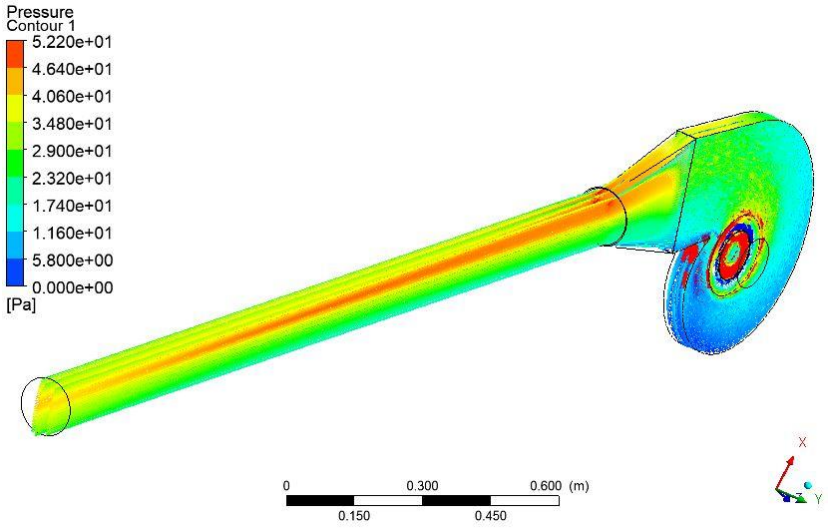

Figure 12. Static Pressure Contour

Flow Patterns on Different Mass Flow Rate

From the low flow coefficient, $\phi = 0.16$, to the high flow coefficient, $\phi = 0.3$, with $\phi = 0.22$ serving as the design point, the flow patterns are discussed for every simulated setting. At the fan's mid-plane, the flow characteristics inside the centrifugal fan were examined. The results of the pressure fluctuation are measured between the volute casing and the impeller's outer circumference. It is apparent in Fig.13 (a) to (h) that the pressure fluctuation affects the eight mass flow rates. The numerical findings show that pressure is dropping and the volume flow rate is rising. This is because a higher mass flow rate also results in an increased air velocity. Consequently, the pressure reduces as a result of this increased volume. It is evident from the simulation findings that low flow rates are where the highest pressure occurs.

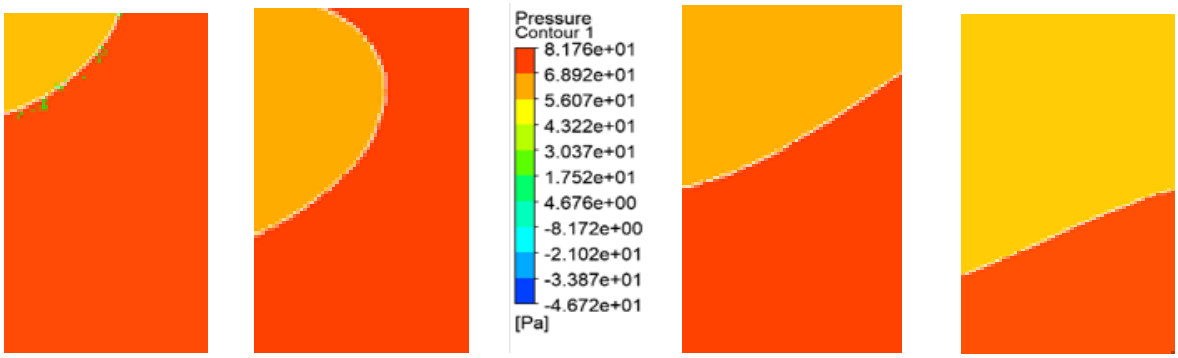

(a) $m^o = 0.0459$ kg/s (b) $m^o = 0.0516$ kg/s (c) $m^o = 0.0574$ kg/s (d) $m^o = 0.0641$ kg/s

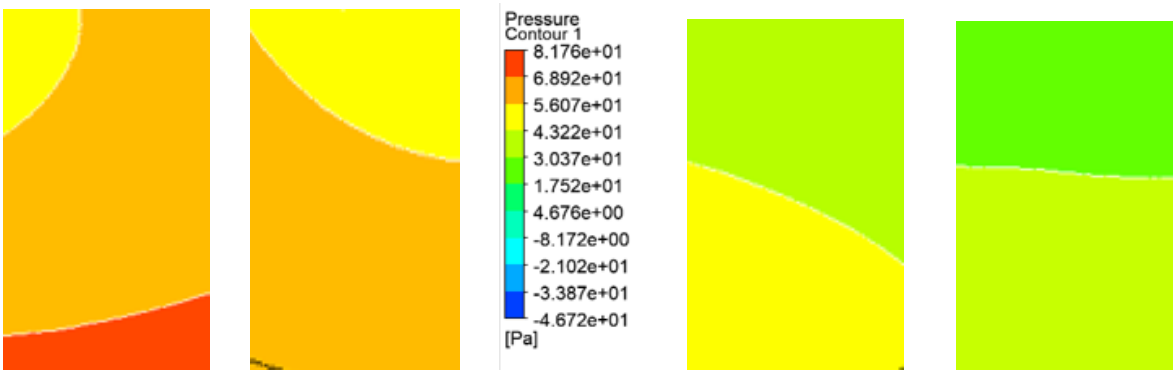

(e) m^o = 0.0689 kg/s (f) m^o = 0.0746 kg/s (g) m^o = 0.0804 kg/s (h) m^o = 0.0861 kg/s

Figure 13. Pressure contours at different mass flow rates

RESULTS AND DISCUSSION

This study presents a numerical simulation, performed with ANSYS CFD-CFX, of the internal movement of a centrifugal fan that is bent backward and is used for ventilation rooms. A detailed analysis of the flow fields inside the fan is demonstrated by the entire system, which includes the fan intake, impeller blades, and volute casing. Numerical simulations were performed on the test fan to illustrate the effects of altering the mass flow rate. Fig. 14, 15, and 16 illustrate the comparison of pressure fluctuation, velocity distribution, static efficiency, and total efficiency for eight different values of mass flow rates. The pressure gradually decreases as the mass flow rates rise in the pressure curve (see Fig. 14). The rate of mass flow increases as the velocity increases in the flow velocity curve (see Fig. 15). The highest static efficiency is 93% and the maximum total efficiency is 96% based on the fan's performance curve (see Fig. 16).

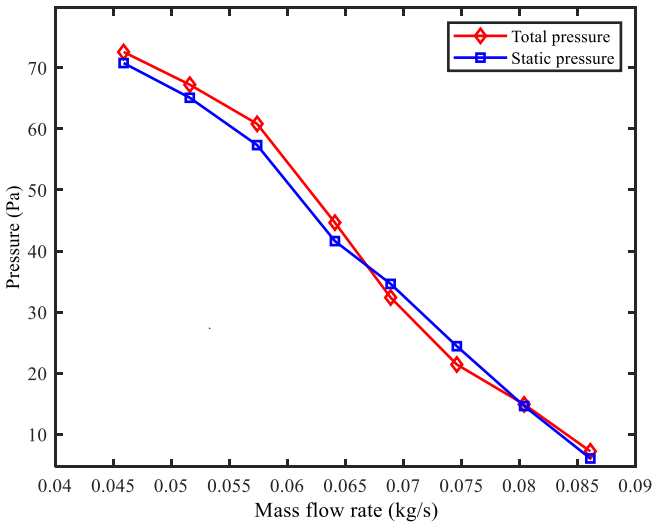

Figure 14. Pressure curve

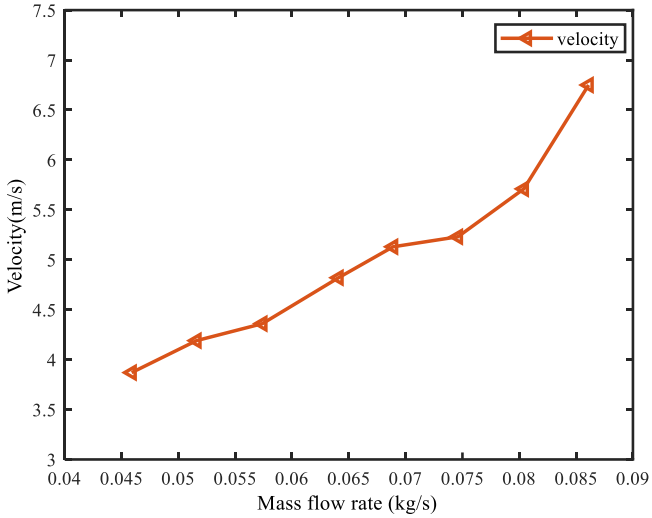

Figure 15. Velocity Curve

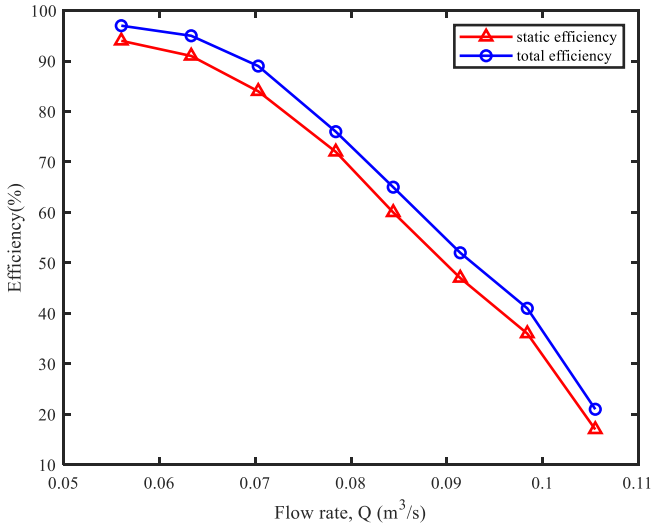

Figure 16. Performance curve

A numerical analysis in three dimensions of the viscous turbulent flow field in the centrifugal fan with a backward curved has been effectively executed. The flow distribution determines the overall flow patterns inside the centrifugal fan. Eight different flow characteristic values were provided, and the efficiency values of each one was examined in this study. The impeller blade pressure and velocity distribution within a centrifugal fan are instantly impacted by changes in the volume flow rate.

CONCLUSION

To sum up, this numerical approach is valid for the investigation of the performance of the backward curved centrifugal fan. That information is one of the keys for the design of centrifugal fan. The new researchers can approach this concept by applying the fan's new design methods. Similar types of computational simulation models can also be applied to analyze the pressure and velocity of the fan, blower, and compressor.

REFERENCES

Abbitt, J., & Lowry, S. (2016). Implementing the digital design process for the development of a centrifugal fan impeller in the undergraduate engineering curriculum. *Procedia Manufacturing*, 5, 1119-1127.

A... J. Stepanoff. (1957). *Centrifugal and axial flow pumps: theory, design, and application*. J. Wiley & Sohn.

Anderson, J.D. & Wendt, J. (1995). Computational fluid dynamics (Vol. 206, p. 332).

Bleier, F. P. (2018). *Fan handbook: selection, application, and design*. McGraw-Hill.

Brahmbhatt, V. & Patel, G. (2014). Performance Enhancement of IND 25 Centrifugal Fan by CFD Analysis. *International Journal of Innovative Research in Science, Engineering and Technology*, 3, 10743-10749.

Chaudhary, S. & Kansal, S. (2013). Performance Analysis of Backward Curved Centrifugal Fan in Heating Ventilation and Air Conditioning. *International Journal of Science and Research*, 2, 170-172.

Gustafson, B., (1989*) Improving Fan System Performance*, Department of Energy, United States.

Gjeta, A. & Malka, L. (2020). Outlet Surface Area Influence in Spiral Casing Design on Centrifugal Fan Performance. *European Journal of Engineering and Technology Research*, 5(1), 37-41.

Huang, C.H. & Hung, M.H. (2013). An optimal design algorithm for centrifugal fans: Theoretical and experimental studies. *Journal of Mechanical Science and Technology*, 27, 761-773.

Liu, X., Dang, Q., & Xi, G. (2008). Performance improvement of centrifugal fan by using CFD. *Engineering Applications of Computational Fluid Mechanics*, 2(2), 130-140.

Samarbakhsh, S. & Alinejad, J. (2011). Experimental and numerical analysis of eight different volutes with the same impeller in a squirrel-cage fan. In *2nd European conference of Control and Mechanical Engineering* (pp. 198-203).

Singh, O. P., Khilwani, R., Sreenivasulu, T., & Kannan, M. (2011). Parametric study of centrifugal fan performance: experiments and numerical simulation. *International Journal of Advances in Engineering & Technology*, 1(2), 33.

Swe, W.W.M., Thu, A.M., Thet, K.C., Htet, Z.M., & Mon, T. (2019). Investigation of Flow Characteristics on Upstream and Downstream of Orifice Using Computational Fluid Dynamics. *International Journal of Mechanical and Mechatronics Engineering*, 13(9), 626-633.

Swe, W.W.M., Morimatsu, H., Hayashi, H., Okumura, T., & Oda, I. (2017). Study of unsteady flow simulation of backward impeller with non-uniform casing. *Journal of Thermal Science*, 26, 208-213.

Wang, J.I.A.B.I.N.G., Ou, Y.I.N.G.D.A., & Wu, K.E.Q.I. (2005). Numerical analysis of internal flow phenomena in a multi-blade centrifugal fan. *TASK Quarterly. Scientific Bulletin of Academic Computer Centre in Gdansk*, 9(2), 245-256.

War, W.M.S. (2017). *Aerodynamic Performance of Backward Centrifugal Fan with Rectangular Casing* (Doctoral dissertation, Nagasaki University (長崎大学)).

White Frank M.: Fluid mechanics, library of congress cataloging in publication Data, 1979.

Yahya, S.M. (2011). *Turbines, Compressors and Fans*. 4th ed. New York: McGraw-Hill Education. https://www.accessengineeringlibrary.com/content/book/9780070

Yokoi, Y. & Inagaki, S. (2005). Experimental Study of Flow Feature in Spiral Casing of Turbo Fan. *Turbo Machinery*, 33, 4.

Yu, Z., Li, S., He, W., Wang, W., Huang, D., & Zhu, Z. (2005). Numerical simulation of flow field for a whole centrifugal fan and analysis of the effects of blade inlet angle and impeller gap. *HVAC&R Research*, 11(2), 263-283